MODELING AND SIMULATION OF OZONE FORMATION FROM A PROPENE-NITROGEN OXIDE-WET AIR MIXTURE IN A SMOG-CHAMBER

Sea Cheon Oh and Yeong-Koo Yeo[†]

Dept. of Chem. Eng., Hanyang University, Seoul 133-791, Korea
(*Received 24 April 1997 • accepted 9 December 1997*)

Abstract – Ozone formation from a propene-nitrogen oxide-wet air mixture was modeled and simulated by using a detailed reaction model to characterize ozone formation in air pollution. Effects of reaction parameters such as light intensity, initial concentrations of propene and nitrogen oxides, temperature and humidity were investigated. The loss reactions of N_2O_5 by H_2O were incorporated in the model developed in the present study. Results of simulations showed good agreement with smog-chamber experimental data. From the results of simulations it was found that the maximum ozone concentration was little affected by humidity. The model proposed in the present study can be used to predict the amount of ozone formation successfully.

Key words: Ozone Formation, Propene, Nitrogen Oxides, Wet-Air Mixture, Modeling

INTRODUCTION

Often the most deleterious air pollutants are not emitted directly by sources but are those formed in the atmosphere by various chemical reactions. In an analysis of air pollution it is therefore necessary to understand the chemical reactions taking place in the atmosphere. The understanding of air pollution chemistry requires identification of the reactions contributing to the chemical dynamics. Thorough investigation of a specific reaction is achieved only when the reaction mechanism is properly specified. Because of the large number of important reactions that take place in the atmosphere, the rapid rates of many of them, and the low concentrations of most reactants, the experimental investigation of air pollution chemistry is very complex and difficult.

To characterize the formation of photochemical smog in air pollution, many recent attempts [Carter et al., 1979a, b; Sakamaki et al., 1982; Fan et al., 1996] have been made to correlate the maximum ozone concentration attained in smog-chamber experiments with the reaction parameters. It is well known that the formation of photochemical smog is influenced by a number of meteorological factors [Carter et al., 1979a, b; Seinfeld, 1986]. Their natural fluctuations contribute to the observed variation in the frequency and the intensity of episodes in different geographic locations and at different times of the year. There has been significant progress recently in understanding the dependences of the photochemical reaction parameters of elementary processes; however, no modeling and simulation experiments concerning the overall reaction parameters' dependence in ozone production have been conducted so far.

This study presents a reaction model which can characterize

ozone formation from a propene-nitrogen oxide-wet air mixture in terms of reaction parameters such as light intensity, initial concentrations of propene and nitrogen oxide, temperature and humidity. The loss reactions of N_2O_5 by H_2O were incorporated in the model developed in the present study. Since a detailed mechanism based on a knowledge of chemical kinetic data for the photooxidation in this system has been reported [Carter et al., 1979a; Sakamaki et al., 1982] recently, it is of great interest to determine whether computer modeling can reproduce the experimentally obtained relationship. For the purpose of establishing an ozone control strategy with the aid of computer simulation, a theoretical prediction is important. Results of simulations based on the reaction model developed in the present study showed good agreement with the experimental data.

MODELING AND COMPUTATIONAL METHOD OF C_3H_6-NO_x-WET AIR MIXTURE

1. Reaction Mechanism

Photochemical reactions are initiated by the absorption of a photon by an atom, molecule, free radical or ion. The oxides of nitrogen, especially NO and NO_2, play an important role in air pollution chemistry. Most of the NO_x formed in combustion is NO. However, NO_2 is formed to some extent from the NO in combustion exhaust gases by

$$2NO + O_2 \rightarrow 2NO_2 \tag{1}$$

Nitrogen dioxide is an important absorber of radiation at the wavelengths prevalent in the atmosphere. Even a small amount of NO_2 present in the atmosphere is sufficient to trigger a complex series of reactions involving organics that lead to photochemical smog. Therefore, NO_2 is the most important air pollutant molecule. When NO and NO_2 are present in sunlight, ozone formation occurs as a result of the photolysis of

---

[†]To whom all correspondence should be addressed.
E-mail: ykyeo@email.hanyang.ac.kr

NO_2,

$$NO_2 + hv \rightarrow NO + O(^3P) \qquad (2)$$

$$O(^3P) + O_2 + M \rightarrow O_3 + M \qquad (3)$$

where M represents N_2 or O_2 or other third molecule that absorbs the excess vibrational energy and thereby stabilizes the O_3 molecule formed. There are no significant sources of ozone in the atmosphere other than reaction (3). Once formed, O_3 reacts with NO to regenerate NO_2,

$$O_3 + NO \rightarrow NO_2 + O_2 \qquad (4)$$

Sakamaki et al. [1982] have considered a dry air system at constant temperature. A wet-air system was considered in this present study, and so the loss reactions of N_2O_5 by H_2O were included in the model. For the simulation of ozone forma-

tion in the C_3H_6-NO_x-wet air mixture according to temperature change, rate constants for the variable temperature were used in this study. The reaction of ozone with propene was postulated to give vibrationally stabilized biradicals (CH_2OO and CH_3CHOO) which react bimolecularly with NO, NO_2, HCHO, and CH_3CHO, and dioxiranes (CH_2OO and CH_3CHOO) which decompose or isomerize unimolecularly. The branching ratios of the unimolecular decay of CH_2OO were taken from the study by Whitten et al. [1980]. The ratio of the atom and radical formation from CH_3CHOO was decreased to 50% of their values [Sakamaki et al., 1982]. The detailed reaction mechanism used in the present study is presented in Table 1. Assuming that known initial concentrations of C_3H_6 and NO_x are placed in a smog-chamber of constant volume, and treating O_2 and M as constant, the rate of the concentration change of O_3 after the irradiation begins is given by

Table 1. List of reactions and rate constants used in the C_3H_6-NO_x-wet air system

Reaction no.	Reaction	Rate constant	Reference
1	$NO_2 + hv \rightarrow NO + O(^3P)$	1.0	a
2	$O_3 + hv \rightarrow O(^1D) + O_2$	2.8×10^{-3}	a
3	$\rightarrow O(^3P) + O_2$	2.0×10^{-2}	b
4	$HONO + hv \rightarrow OH + NO$	1.5×10^{-1}	c
5	$H_2O_2 + hv \rightarrow 2OH$	4.9×10^{-4}	b
6	$NO_3 + hv \rightarrow NO + O_2$	4.3	d
7	$\rightarrow NO_2 + O(^3P)$	1.3×10^1	d
8	$HCHO + hv \rightarrow H + HCO$	2.0×10^{-3}	b
9	$\rightarrow H_2 + CO$	6.3×10^{-3}	b
10	$CH_3CHO + hv \rightarrow CH_3 + HCO$	2.6×10^{-3}	e
11	$C_2H_5CHO + hv \rightarrow C_2H_5 + HCO$	2.6×10^{-3}	b
12	$CH_3COCHO + hv \xrightarrow{O_2} CH_3C(O)O_2 + HCO$	1.5×10^{-1}	b
13	$CH_3COCH_2OH + hv \xrightarrow{O_2} CH_3C(O)O_2 + CH_2OH$	9.0×10^{-4}	b
14	$CH_3CH(OH)CHO + hv \rightarrow CH_3CHOH + HCO$	2.6×10^{-3}	b
15	$CH_2CO + hv \xrightarrow{O_2} CH_2O_2 + CO$	2.4×10^{-3}	b
16	$\xrightarrow{O_2} \text{CH}_2\text{OO} + CO$	9.7×10^{-3}	b
17	$CH_3ONO + hv \rightarrow CH_3O + NO$	1.3×10^{-1}	b
18	$C_2H_5ONO + hv \rightarrow C_2H_5O + NO$	1.3×10^{-1}	b
19	$O(^3P) + O_2 + M \rightarrow O_3 + M$	$6.0 \times 10^{-3}(T/300)^{-2.3}$	a
20	$O(3P) + NO_2 \rightarrow NO + O_2$	9.3×10^{-12}	a
21	$O(^3P) + NO_2 + M \rightarrow NO_3 + M$	1.0×10^{-31}	b
22	$O(^3P) + NO + M \rightarrow NO_2 + M$	1.1×10^{-31}	b
23	$O(^3P) + O_3 \rightarrow 2O_2$	9.6×10^{-15}	b
24	$O(^1D) + M \rightarrow O(^3P) + M$	2.9×10^{-11}	a
25	$O(^1D) + H_2O \rightarrow 2OH$	2.2×10^{-10}	a
26	$O(^1D) + O_3 \rightarrow 2O_2$	2.4×10^{-10}	b
27	$O_3 + NO \rightarrow NO_2 + O_2$	$2.2 \times 10^{-12} \exp(-1430/T)$	a
28	$O_3 + NO_2 \rightarrow NO_3 + O_2$	$1.2 \times 10^{-13} \exp(-2450/T)$	a
29	$O_3 + OH \rightarrow HO_2 + O_2$	$1.6 \times 10^{-12} \exp(-940/T)$	a
30	$O_3 + HO_2 \rightarrow OH + 2O_2$	$3.1 \times 10^{-12} \exp(-187/T)$	a
31	$2NO + O_2 \rightarrow 2NO_2$	$3.3 \times 10^{-39} \exp(530/T)$	a
32	$NO + NO_3 \rightarrow 2NO_2$	2.0×10^{-11}	a
33	$NO + OH \rightarrow HONO$	6.6×10^{-12}	a
34	$NO + HO_2 \rightarrow OH + NO_2$	$3.7 \times 10^{-12} \exp(240/T)$	a
35	$NO_2 + NO_3 \rightarrow N_2O_5$	$4.7 \times 10^{-13} \exp(259/T)$	a

Table 1. Continued

Reaction no.	Reaction	Rate constant	Reference
36	$N_2O_5 \rightarrow NO_2+NO_3$	$2.0 \times 10^{14} \exp(-10660/T)$	a
37	$NO_2+OH \rightarrow HNO_3$	1.1×10^{-11}	a
38	$NO_2+HO_2 \rightarrow HO_2NO_2$	1.4×10^{-12}	a
39	$HO_2NO_2 \rightarrow HO_2+NO_2$	$1.3 \times 10^{14} \exp(-10418/T)$	a
40	$HO_2+HO_2 \rightarrow H_2O_2+O_2$	$[2.2 \times 10^{-13} \exp(620/T)+1.9 \times 10^{-33}[M]$ $\exp(980/T)] \times [1+1.4 \times 10^{-21}[H_2O]$ $\exp(2200/T)]$	a
41	$H_2O_2+OH \rightarrow HO_2+H_2O$	$3.1 \times 10^{-12} \exp(-187/T)$	a
42	$CO+OH \rightarrow H+CO_2$	3.0×10^{-13}	b
43	$H+O_2+M \rightarrow HO_2+M$	1.7×10^{-32}	b
44	$NO+NO_2+H_2O \rightarrow 2HNO_3$	4.4×10^{-40}	a
45	$N_2O_5+H_2O \rightarrow 2HNO_3$	2.0×10^{-21}	a
46	$O_3 \rightarrow O_3$ (wall)	1.1×10^{-5}	b
47	$NO_2 \rightarrow NO_2$ (wall)	7.2×10^{-6}	b
48	$C_3H_6+O(^3P) \rightarrow C_2H_5+HCO$	2.3×10^{-12}	b
49	$\rightarrow CH_3CHCH_2O$	1.1×10^{-12}	b
50	$\rightarrow C_2H_5CHO$	1.1×10^{-12}	b
51	$HCO+O_2 \rightarrow HO_2+CO$	fast	a
52	$CH_3+O_2 \rightarrow CH_3O_2$	fast	b
53	$C_2H_5+O_2 \rightarrow C_2H_5O_2$	fast	b
54	$CH_3O_2+NO \rightarrow CH_3O+NO_2$	$4.2 \times 10^{-12} \exp(180/T)$	a
55	$C_2H_5O_2+NO \rightarrow C_2H_5O+NO_2$	$4.2 \times 10^{-12} \exp(180/T)$	a
56	$CH_3O_2+NO_2 \rightarrow CH_3O_2NO_2$	4.0×10^{-12}	a
57	$CH_3O_2NO_2 \rightarrow CH_3O_2+NO_2$	1.0×10^1	f
58	$C_2H_5O_2+NO_2 \rightarrow C_2H_5O_2NO_2$	1.3×10^{-11}	f
59	$C_2H_5O_2NO_2 \rightarrow C_2H_5O_2+NO_2$	1.0×10^1	f
60	$CH_3O_2+HO_2 \rightarrow CH_3OOH+O_2$	2.9×10^{-12}	f
61	$C_2H_5O_2+HO_2 \rightarrow C_2H_5OOH+O_2$	2.9×10^{-12}	f
62	$2CH_3O_2 \rightarrow 2CH_3O+O_2$	1.6×10^{-13}	b
63	$\rightarrow CH_3OH+HCHO+O_2$	2.7×10^{-13}	b
64	$\rightarrow CH_3OOCH_3$	3.0×10^{-14}	b
65	$2C_2H_5O_2 \rightarrow C_2H_5OOC_2H_5$	4.5×10^{-14}	b
66	$CH_3O+NO \rightarrow CH_3ONO$	1.7×10^{-11}	f
67	$\rightarrow HCHO+HNO$	3.0×10^{-12}	f
68	$C_2H_5O \rightarrow C_2H_5ONO$	1.7×10^{-11}	f
69	$\rightarrow CH_3CHO+HNO$	3.0×10^{-12}	f
70	$CH_3O+NO_2 \rightarrow CH_3ONO_2$	1.4×10^{-11}	f
71	$\rightarrow HCHO+HNO$	2.4×10^{-12}	f
72	$C_2H_5O+NO_2 \rightarrow C_2H_5ONO_2$	1.4×10^{-11}	f
73	$\rightarrow CH_3CHO+HNO$	2.4×10^{-12}	f
74	$CH_3+O_2 \rightarrow HCHO+HO_2$	6.8×10^{-16}	b
75	$C_2H_5O+O_2 \rightarrow CH_3CHO+HO_2$	6.8×10^{-16}	b
76	$CH_3C(O)O_2+NO \rightarrow CH_3+CO_2+NO_2$	$4.2 \times 10^{-12} \exp(180/T)$	a
77	$CH_3C(O)O_2+NO_2 \rightarrow CH_3C(O)O_2NO_2$	4.7×10^{-12}	a
78	$CH_3C(O)O_2NO_2 \rightarrow CH_3C(O)O_2+NO_2$	$1.95 \times 10^{16} \exp(-13543/T)$	a
79	$CH_3C(O)_2+HO_2 \rightarrow CH_3C(O)O_2H+O_2$	3.0×10^{-12}	f
80	$C_2H_5C(O)O_2+NO \rightarrow C_2H_5+CO_2+NO_2$	2.0×10^{-11}	f
81	$C_2H_5C(O)O_2+NO_2 \rightarrow C_2H_5C(O)O_2NO_2$	1.3×10^{-11}	f
82	$C_2H_5C(O)O_2NO_2 \rightarrow C_2H_5C(O)O_2+NO_2$	$1.95 \times 10^{16} \exp(-13543/T)$	a
83	$C_2H_5C(O)O_2+HO_2 \rightarrow C_2H_5C(O)O_2H+O_2$	3.0×10^{-12}	f
84	$C_3H_6+O_3 \rightarrow CH_3CHO_2^*+HCHO$	5.5×10^{-18}	b
85	$\rightarrow CH_3CHO+CH_2O_2^*$	5.5×10^{-18}	b
86	$CH_2O_2^* \rightarrow CH_2O_2$	(0.5)	b
87	$\rightarrow CH_2OO$	(0.5)	b
88	$CH_3CHO_2^* \rightarrow CH_3CHO_2$	(0.5)	b
89	$\rightarrow CH_3CHOO$	(0.5)	b
90	$CH_2O_2+NO \rightarrow HCHO+NO_2$	1.9×10^{-11}	f
91	$CH_3CHO_2+NO \rightarrow CH_3CHO+NO_2$	1.9×10^{-11}	f

Table 1. Continued

Reaction no.	Reaction	Rate constant	Reference
92	$CH_2O_2+NO_2 \rightarrow HCHO+NO_3$	2.0×10^{-12}	g
93	$CH_3CHO_2+NO_2 \rightarrow CH_3CHO+NO_3$	2.0×10^{-12}	g
94	$CH_2O_2+HCHO \rightarrow$ product	1.4×10^{-13}	b
95	$CH_2O_2+CH_3CHO \rightarrow$ product	1.4×10^{-13}	b
96	$CH_3CHO_2+HCHO \rightarrow$ product	7.0×10^{-13}	adj
97	$CH_3CHO_2+CH_3CHO \rightarrow$ product	7.0×10^{-13}	adj
98	$\overline{CH_2OO} \rightarrow H_2+CO_2$	(0.18)	b
99	$\rightarrow CO+H_2O$	(0.67)	b
100	$\rightarrow 2H+CO_2$	(0.09)	b
101	$\rightarrow HCHO$	(0.06)	b
102	$CH_3\overline{CHOO} \rightarrow CH_4+CO_2$	(0.24)	b
103	$\rightarrow CH_3+CO+OH$	(0.27)	b
104	$\rightarrow CH_3+H+CO_2$	(0.35)	b
105	$\rightarrow CH_3O+H+CO$	(0.06)	b
106	$\rightarrow CH_2CO+H_2O$	(0.08)	b
107	$C_3H_6+OH \xrightarrow{O_2} CH_3CH(O_2)CH_2OH$	1.6×10^{-11}	f
108	$C_3H_6+OH \xrightarrow{O_2} CH_3CH(O_2)CH_2OH$	8.6×10^{-12}	f
109	$CH_3CH(O_2)CH_2OH+NO \rightarrow CH_3CH(O)CH_2OH+NO_2$	1.9×10^{-11}	f
110	$\rightarrow CH_3CH(ONO_2)CH_2OH$	3.6×10^{-13}	adj
111	$CH_3CH(OH)CH_2O_2+NO \rightarrow CH_3CH(OH)CH_2O+NO_2$	1.9×10^{-11}	f
112	$\rightarrow CH_3CH(OH)CH_2ONO_2$	3.6×10^{-13}	adj
113	$CH_3CH(O_2)CH_2OH+NO_2 \rightarrow CH_3CH(O_2NO_2)CH_2OH$	1.3×10^{-11}	f
114	$CH_3CH(O_2NO_2)CH_2OH \rightarrow CH_3CH(O_2)CH_2OH+NO_2$	1.0×10^{1}	f
115	$CH_3CH(OH)CH_2O_2+NO_2 \rightarrow CH_3CH(OH)CH_2O_2NO_2$	1.3×10^{-11}	f
116	$CH_3CH(OH)CH_2O_2NO_2 \rightarrow CH_3CH(OH)CH_2O_2+NO_2$	1.0×10^{1}	f
117	$CH_3CH(O)CH_2OH \rightarrow CH_3CHO+CH_2OH$	2.3×10^{6}	adj
118	$CH_3C(OH)CH_2O \rightarrow CH_3CHOH+HCHO$	4.0×10^{5}	adj
119	$CH_2OH+O_2 \rightarrow HCHO+HO_2$	fast	b
120	$CH_3CHOH+O_2 \rightarrow CH_3CHO+HO_2$	fast	b
121	$CH_3CH(O)CH_2OH+O_2 \rightarrow CH_3C(O)CH_2OH+HO_2$	1.2×10^{-15}	f
122	$CH_3CH(OH)CH_2O+O_2 \rightarrow CH_3CH(OH)CHO+HO_2$	1.2×10^{-15}	f
123	$CH_3CH(O_2)CH_2OH+HO_2 \rightarrow CH_3CH(O_2H)CH_2OH+O_2$	2.9×10^{-12}	f
124	$CH_3CH(OH)CH_2O_2+HO_2 \rightarrow CH_3CH(OH)CH_2O_2H+O_2$	2.9×10^{-12}	f
125	$CH_3C(O)CH_2OH+OH \rightarrow CH_3C(O)CHOH+H_2O$	7.0×10^{-12}	f
126	$CH_3C(O)CHOH+O_2 \rightarrow CH_3C(O)CHO+HO_2$	fast	b
127	$CH_3CH(OH)CHO+OH \rightarrow CH_3C(OH)CHO+H_2O$	1.3×10^{-11}	f
128	$CH_3C(OH)CHO+O_2 \rightarrow CH_3C(O)CHO+HO_2$	fast	b
129	$CH_3CH(OH)CHO+OH \rightarrow CH_3CH(OH)CO+H_2O$	1.6×10^{-11}	f
130	$CH_3CH(OH)CO+O_2 \rightarrow CH_3CH(OH)C(O)O_2$	fast	b
131	$CH_3CH(OH)C(O)O_2+NO \rightarrow CH_3CH(OH)CO_2+NO_2$	2.0×10^{-11}	f
132	$CH_3CH(OH)CO_2 \rightarrow CH_3CHOH+CO_2$	fast	b
133	$CH_3CH(OH)C(O)O_2+NO_2 \rightarrow CH_3CH(OH)C(O)O_2NO_2$	1.3×10^{-11}	f
134	$CH_3CH(OH)C(O)O_2NO_2 \rightarrow CH_3CH(OH)C(O)O_2+NO_2$	8.0×10^{-4}	f
135	$CH_3C(O)CHO+OH \rightarrow CH_3C(O)CO+H_2O$	1.6×10^{-11}	f
136	$CH_3C(O)CO \rightarrow CH_3CO+CO$	fast	b
137	$C_3H_6+NO_3 \xrightarrow{O_2} CH_3CH(O_2)CH_2ONO_2$	5.5×10^{-15}	f
138	$\xrightarrow{O_2} CH_3CH(ONO_2)CH_2O_2$	2.7×10^{-15}	f
139	$CH_3CH(O_2)CH_2ONO_2+NO \rightarrow CH_3CH(O)CH_2ONO_2+NO_2$	1.9×10^{-11}	f
140	$\rightarrow CH_3CH(ONO_2)CH_2ONO_2$	3.6×10^{-12}	adj
141	$CH_3CH(ONO_2)CH_2O_2+NO \rightarrow CH_3CH(ONO_2)CH_2O+NO_2$	1.9×10^{-11}	f
142	$\rightarrow CH_3CH(ONO_2)CH_2ONO_2$	3.6×10^{-12}	adj
143	$CH_3CH(O_2)CH_2ONO_2+NO_2 \rightarrow CH_3CH(O_2NO_2)CH_2ONO_2$	1.3×10^{-11}	f
144	$CH_3CH(O_2NO_2)CH_2ONO_2 \rightarrow CH_3CH(O_2)CH_2ONO_2+NO_2$	1.0×10^{1}	f
145	$CH_3CH(ONO_2)CH_2O_2+NO_2 \rightarrow CH_3CH(ONO_2)CH_2O_2NO_2$	1.3×10^{-11}	f

Table 1. Continued

Reaction no.	Reaction	Rate constant	Reference
146	$CH_3CH(ONO_2)CH_2O_2NO_2 \rightarrow CH_3CH(ONO_2)CH_2O_2+NO_2$	1.0×10^1	f
147	$CH_3CH(O_2)CH_2ONO_2+HO_2 \rightarrow CH_3CH(OOH)CH_2ONO_2+O_2$	2.9×10^{-12}	f
148	$CH_3CH(ONO_2)CH_2O+HO_2 \rightarrow CH_3CH(ONO_2)CH_2OOH+O_2$	2.9×10^{-12}	f
149	$CH_3CH(O)CH_2ONO_2+NO_2 \rightarrow CH_3CH(ONO_2)CH_2ONO_2$	1.4×10^{-11}	f
150	$CH_3CH(ONO_2)CH_2O+NO_2 \rightarrow CH_3CH(ONO_2)CH_2ONO_2$	1.4×10^{-11}	f
151	$CH_3CH(O)CH_2ONO_2+O_2 \rightarrow CH_3C(O)CH_2ONO_2+H_2O$	3.0×10^{-18}	b
152	$CH_3CH(ONO_2)CH_2O+O_2 \rightarrow CH_3CH(ONO_2)CHCHO+HO_2$	3.0×10^{-18}	b
153	$CH_3CH(O)CH_2ONO_2 \rightarrow CH_3CHO+HCHO+NO_2$	3.1×10^5	b
154	$CH_3CH(ONO_2)CH_2O \rightarrow CH_3CHO+HCHO+NO_2$	3.0×10^1	b
155	$HCHO+OH \rightarrow HCO+H_2O$	9.4×10^{-12}	f
156	$CH_3CHO+OH \xrightarrow{O_2} CH_3CO(O_2)+H_2O$	1.6×10^{-11}	f
157	$C_2H_5CHO+OH \xrightarrow{O_2} C_2H_5CO(O_2)+H_2O$	1.6×10^{-11}	f
158	$HCHO+NO_3 \rightarrow HCO+HNO_3$	1.8×10^{-15}	f
159	$CH_3CHO+NO_3 \xrightarrow{O_2} CH_3CO(O_2)+HNO_3$	2.0×10^{-15}	f
160	$C_2H_5CHO+NO_3 \xrightarrow{O_2} C_2H_5CO(O_2)+HNO_3$	2.0×10^{-15}	f

a: Seinfeld, 1986, b: Sakamaki et al., 1982, c: Stockwell and Calvert, 1978, d: Graham and Johnston, 1978, e: Weaver et al., 1977, f: Carter et al., 1979a, g: Whitten et al., 1977, adj: adjust

$$\frac{d[O_3]}{dt} = k_{19}[O(^3P)][O_2][M] - \{k_2[O_3] + k_3[O_3]$$
$$+ k_{23}[O(^3P)][O_3] + k_{26}[O(^1D)][O_3] + k_{27}[O_3][NO]$$
$$+ k_{28}[O_3][NO_2] + k_{29}[O_3][OH] + k_{30}[O_3][HO_2] + k_{46}[O_3]$$
$$+ k_{84}[C_3H_6][O_3] + k_{85}[C_3H_6][O_3]\} \tag{5}$$

The dynamic equations for the other reactants can be written, just as we have done for O_3. In Table 1 the values in parentheses are branching ratios normalized to unity and the photolysis rate constants are the relative rates to that of NO_2. The mechanisms presented in Table 1 are based on those reported by Sakamaki et al. [1982] with some modifications.

2. Smog-Chamber Experiments and Computational Method

The experimental facilities and methods employed in these smog chamber experiments are discussed in detailed elsewhere [Carter et al., 1979b; Sakamaki et al., 1982] and are only briefly described here. The evacuable thermostated chamber consists of a 5800-L cylindrical aluminum alloy cell coated on the inside with Teflon and equipped with quartz end windows. Photolysis was performed with a 25000 W solar simulator producing a collimated beam designed to minimize direct irradiation of the chamber walls. The temperature control system was designed to regulate the temperature of chamber walls to $\pm 0.5°C$ over the -20 to $+100°C$ range. In this system ethylene glycol is heated or cooled by external heat exchangers and then circulated by means of a 1.5 hp pump through channels welded to the chamber exterior. A 10-kW electrical heater powers the exchanger used for the heating cycle, and a 7.5-ton two-stage refrigeration unit is used for the cooling cycle. The chamber walls are insulated with 1 in. of fiberglass insulation and 2 in. of polyurethane foam and are covered with an aluminum sheath. Prior to each experiment, the chamber was evacuated to at least 10^{-4} Torr. After the chamber was filled with purified matrix air [Carter et al., 1979b] at the de-

sired temperature and relative humidity, reactants were added and allowed to mix for at least 30 min. Ozone, NO, NO_2, and NO_x were monitored by chemiluminescence method, and CO and organics by gas chromatography.

For computation the concentration of water vapor must be in units of ppm. For a given ambient temperature T, relative humidity RH is defined as the ratio of the partial pressure of water to its saturation vapor pressure at the same temperature. Alternatively, RH is the ratio of the actual mole fraction of water vapor y to that at saturation, y_s,

$$RH = 100 \frac{y}{y_s} \tag{6}$$

where the factor 100 is used because RH is usually expressed in percent. Since the mole fraction is equivalent to the volume fraction, the water concentration in ppm is given by

$$[H_2O] = 10^6 y = 10^4 RH \, y_s \text{ (ppm)} \tag{7}$$

This equation can be written in terms of $p^0_{H_2O}$ and the atmospheric pressure p,

$$[H_2O] = 10^4 RH \frac{p^0_{H_2O}}{p} \text{ (ppm)} \tag{8}$$

In order to evaluate this expression, the saturation vapor pressure must be known. McRae [1980] suggested the following expression for $p^0_{H_2O}$;

$$p^0_{H_2O}(T) = p_s \exp[13.3185a - 1.9760a^2 - 0.6445a^3 - 0.1299a^4] \tag{9}$$

where p_s is the standard atmospheric pressure of 1013.25 mb, and the parameter a is defined in terms of the ambient T(K) and the steam temperature $T_s=373.15$ K at p_s,

$$a = 1 - \frac{T_s}{T} = \frac{T - 373.15}{T} \tag{10}$$

The experimental data presented by Sakamaki et al. [1982] and Carter et al. [1979b] were used to evaluate the results of simulations based on the present reaction models. Curve fitting of the experimental data and the simulation results was attempted for the C_3H_6 (3.05 ppm)-NO(1.477 ppm)-NO_2(0.023 ppm)-dry air run. Fitting to the time profiles of NO, NO_2, C_3H_6 and O_3, as well as to the maximum O_3 level, was attempted as a first priority. The trials were made by adjusting the reaction rate constant. Calculations were performed on an IBM PC 586 computer by using the 4th Runge-Kutta method for the integration of coupled differential equations.

RESULTS AND DISCUSSION

The initial conditions for each simulation are given in Table 2 together with experimental and simulated results for $[O_3]_{max}$. Fig. 1 shows the time profile of each species simulated using the present reaction model for the C_3H_6 (3.05 ppm)-NO (1.477 ppm)-NO_2 (0.023 ppm)-dry air run. Initial conditions used for the simulation are the same as those for the experiment. A slight discrepancy in the simulation as compared to the experimental data can be noted in Fig. 1. Such a discrepancy was reported as a result of the unknown radical source of OH and HO_2 [Carter et al., 1979a]. However, in this study, the hypothetical radical source was not included since there was little discrepancy between the simulation and the experiment. A comparison of $[O_3]_{max}$ in the C_3H_6-NO_x-wet air mixture obtained by simulations and experiments according to $[C_3H_6]_0$, $[NO_x]_0$, k_1, and humidity is shown in Table 2 and Figs. 2-5. Fig. 2 shows that the $[O_3]_{max}$ increases when $[NO_x]_0$ is increased, keeping $[C_3H_6]_0$ constant, and there is little discrepancy between the
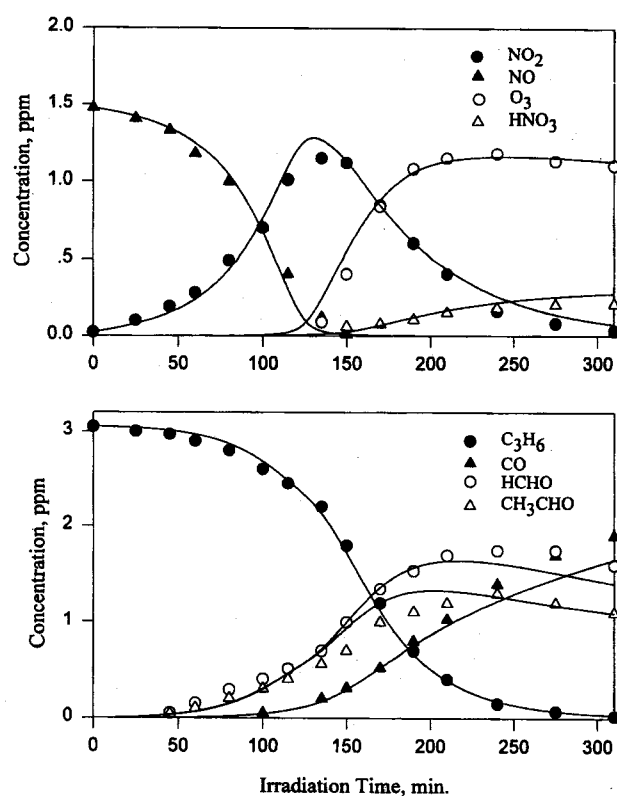

Fig. 1. The comparison of simulated (lines) and experimental (symbols) concentrations for the C_3H_6-NO_x-wet air system, run no. 1 in Table 2.

simulation and the experiment. In Fig. 3, it was found that the $[O_3]_{max}$ could be calculated according to $[C_3H_6]_0$, although

Table 2. Experimental and simulated results for Irradiation of the C_3H_6-NO_x-wet air System

| Run no.	Run conditions					Experimental $[O_3]_{max}$, ppm	Calculated $[O_3]_{max}$, ppm
	Temp. (°C)	Initial concn., ppm			Light inten. k_1, min^{-1}	RH %		
		C_3H_6	NO	NO_2				
1	30	3.05	1.477	0.023	0.27	dry air	1.180	1.161
2	30	0.50	0.004	0.041	0.16	dry air	0.151	0.145
3	30	0.50	0.008	0.082	0.16	dry air	0.236	0.236
4	30	0.50	0.011	0.176	0.16	dry air	0.363	0.367
5	30	0.50	0.255	0.035	0.16	dry air	0.443	0.463
6	30	0.05	0.003	0.035	0.16	dry air	0.085	0.105
7	30	0.20	0.004	0.036	0.16	dry air	0.136	0.129
8	30	0.30	0.005	0.034	0.16	dry air	0.136	0.138
9	30	0.40	0.005	0.035	0.16	dry air	0.139	0.141
10	30	0.50	0.012	0.073	0.37	dry air	0.390	0.372
11	30	0.50	0.012	0.078	0.31	dry air	0.366	0.359
12	30	0.50	0.009	0.074	0.25	dry air	0.307	0.311
13	30	0.50	0.009	0.079	0.19	dry air	0.271	0.284
14	30	0.50	0.007	0.082	0.13	dry air	0.232	0.235
15	30	0.10	0.004	0.032	0.16	dry air	0.106	0.130
16	30	0.10	0.004	0.032	0.16	20	-	0.130
17	30	0.10	0.004	0.032	0.16	40	-	0.129
18	30	0.10	0.004	0.032	0.16	60	-	0.128
19	16.1	9.50	3.960	1.880	0.38	11	2.340	2.388
20	32.8	10.1	4.150	1.880	0.38	5.0	2.423	2.395
21	50.5	10.64	4.740	1.870	0.39	2.0	2.050	2.116
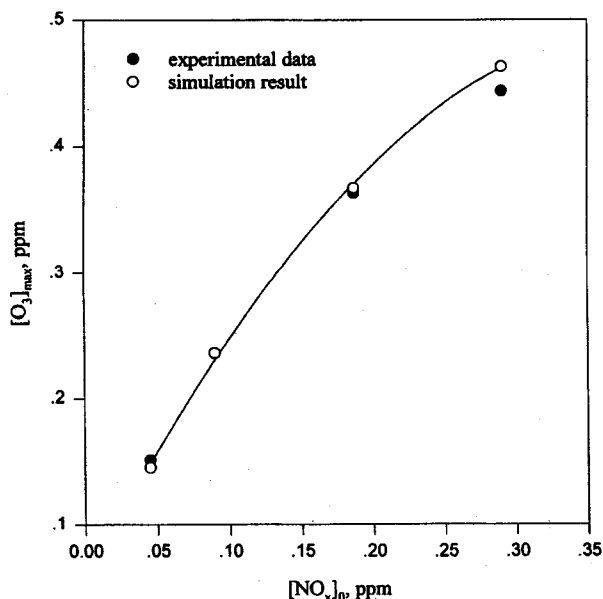
Fig. 2. The comparison of simulated and experimental $[O_3]_{max}$ for the change of $[NO_x]_0$, run no. 2, 3, 4 and 5 in Table 2.

Fig. 4. The comparison of simulated and experimental $[O_3]_{max}$ for the change of light intensity, run no. 10, 11, 12, 13 and 14 in Table 2.

there is a slight disagreement between the simulation and experiment which might be due to the experimental error in the low-concentration runs. Fig. 4 shows a comparison of simulated and experimental $[O_3]_{max}$ when the light intensity, k_1, is changed keeping $[C_3H_6]_0$, $[NO_x]_0$ constant. As can be seen, the proportional relationship between the $[O_3]_{max}$ and k_1 has been well reproduced. Fig. 5 shows the results of simulations for the change of humidity. From the results of simulations it was found that the rates of O_3 formation increase with increasing humidity, but the $[O_3]_{max}$ concentration was little affected by humidity. Although the experimental data were in-
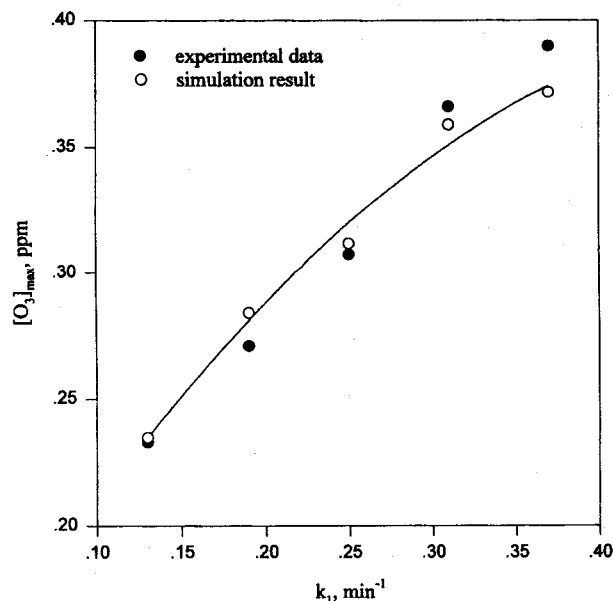
sufficient to determine whether the variation in humidity has a significant effect, preliminary results of simulation performed in this work suggest that humidity effects are small compared to those of the other reaction parameters, at least for the propene-nitrogen oxide-wet air mixture. Fig. 6 shows the time profiles of O_3 simulated using the present reaction model for the change of temperature, $T \geq 16\,^{\circ}C$. From Fig. 6 we can see that the rates of O_3 formation increase with increasing temperature, while the $[O_3]_{max}$ concentration was relatively unaffected by temperature. The rate of formation of O_3 could not be predicted precisely by the present model due to insufficient experimental kinetic data. But the computed concentration of
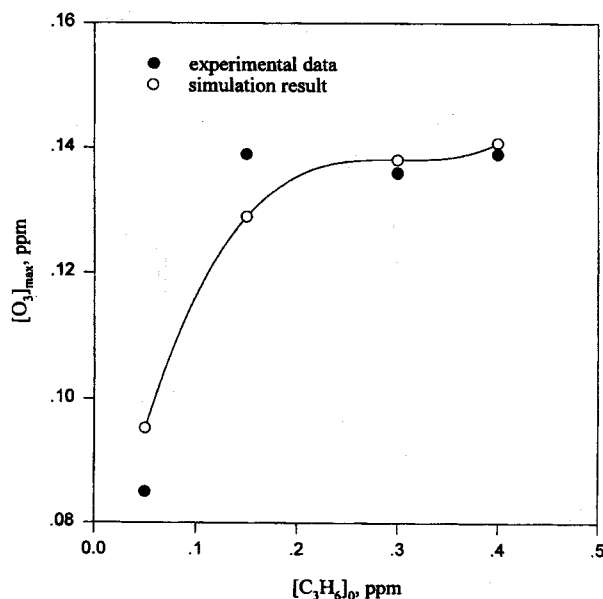

Fig. 3. The comparison of simulated and experimental $[O_3]_{max}$ for the change of $[C_3H_6]_0$, run no. 6, 7, 8 and 9 in Table 2.
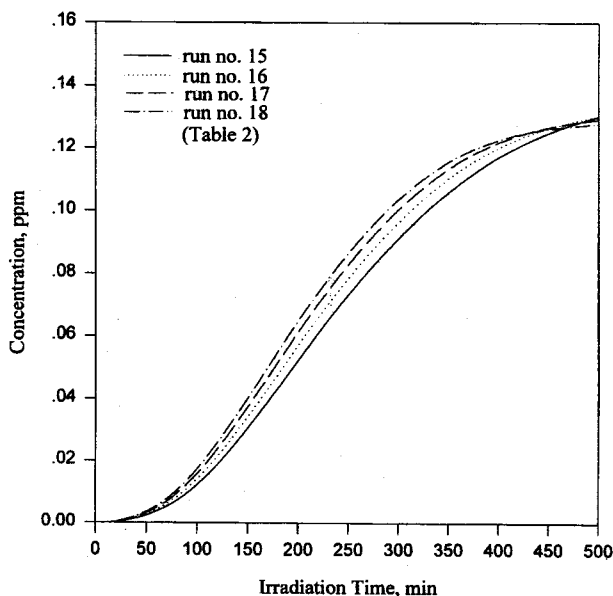

Fig. 5. The simulation results of the rates of O_3 formation for the change of humidity.
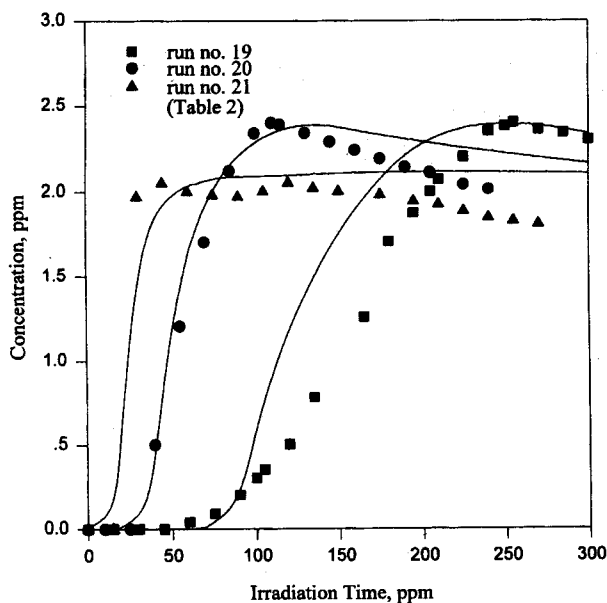
Fig. 6. The comparison of simulated (lines) and experimental (symbols) rates of O_3 formation for the change of temperature.

$[O_3]_{max}$ showed good agreement with the experimental value.

CONCLUSION

The modeling and simulation of the C_3H_6-NO_x-wet air mixture was performed by using a detailed reaction model considering the effect of temperature and the loss reactions of N_2O_5 by H_2O in order to characterize O_3 formation in air pollution. From the results of simulations it was found that the reaction model developed in the present study can be used to predict the amounts of O_3 formation successfully. Although the photochemical models presented in this study took into account the effects of temperature and humidity on photochemical ozone formation, the predictive capabilities of the models concerning these effects do not appear to be totally satisfactory, and they may have errors in important areas relating to

temperature effects. Further basic studies of the temperature and humidity dependences of the photochemical reaction mechanisms are required to improve the effectiveness of the photochemical models.

REFERENCES

Carter, W. P. L., Lloyd, A. C., Sprung, J. L and Pitts, J. N. Jr., "An Experimental Investigation of Chamber-Dependent Radical Sources", *Int. J. Chem. Kinet.*, **11**, 45 (1979a).

Carter, W. P. L., Winer, A. M., Darnal, K. R. and Pitts, J. N. Jr., "Smog Chamber Studies of Temperature Effects in Photochemical Smog", *Environ. Sci. Technol.*, **13**, 1094 (1979b).

Fan, Z., Kamens, R. M., Zhang, J. and Hu, J., "Ozone-Nitrogen Dioxide-NPAH Heterogeneous Soot Particle Reactions and Modeling NPAH in the Atmosphere", *Environ. Sci. Technol.*, **30**, 2821 (1996).

Graham, R. A. and Johnston, H. S., "The Photochemistry of NO_3 and the Kinetics of the N_2O_5-O_3 System", *J. Phys. Chem.*, **82**, 254 (1978).

McRae, G. J., "A Simple Procedure for Calculating Atmospheric Water Vapor Concentration", *J. Air Pollution Control Assoc.*, **30**, 394 (1980).

Sakamaki, F., Okuda, M., Akimoto, H. and Yamazaki, H., "Computer Modeling Study of Photochemical Ozone Formation in the Propene-Nitrogen Oxides-Dry Air System. Generalized Maximum Ozone Isopleth", *Environ. Sci. Technol.*, **16**, 45 (1982).

Seinfeld, J. H., "Atmospheric Chemistry and Physics of Air Pollution", John Wiley & Sons, New York (1986).

Stockwell, W. R. and Calvert, J. G., "The Near Ultraviolet Absorption Spectrum of Gaseous HONO and N_2O_3", *J. Photochem.*, **8**, 193 (1978).

Weaver, J., Meagher, J. and Heicklen, J., "Photooxidation of CH_3CHO Vapor at 3130 A", *J. Photochem.*, **6**, 111 (1977).

Whitten, G. Z., Killus, J. P. and Hogo, H., "Modeling of Simulated Photochemical Smog with Kinetics Mechanisms", Final Report, EPA-600/3-80-028a, **1** (1980).